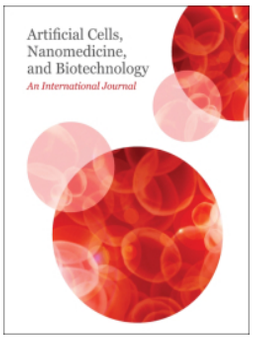

Taylor & Francis
Taylor & Francis Group

Artificial Cells, Nanomedicine, and Biotechnology

An International Journal

ISSN: (Print) (Online) Journal homepage: informahealthcare.com/journals/ianb20

Molecular transport network security using multi-wavelength optical spins

Surachai Tunsiri, Nopparat Thammawongsa, Somsak Mitatha & Preecha P. Yupapin

To cite this article: Surachai Tunsiri, Nopparat Thammawongsa, Somsak Mitatha & Preecha P. Yupapin (2016) Molecular transport network security using multi-wavelength optical spins, Artificial Cells, Nanomedicine, and Biotechnology, 44:1, 240-247, DOI: 10.3109/21691401.2014.940083

To link to this article: https://doi.org/10.3109/21691401.2014.940083

Published online: 24 Jul 2014.

Artificial Cells, Nanomedicine, and Biotechnology, 2016; 44: 240–247

ISSN: 2169-1401 print / 2169-141X online
DOI: 10.3109/21691401.2014.940083

Taylor & Francis
Taylor & Francis Group

Molecular transport network security using multi-wavelength optical spins

Surachai Tunsiri, Nopparat Thammawongsa, Somsak Mitatha & Preecha P. Yupapin

Advanced Studies center, Faculty of Science, King Mongkut's Institute of Technology Ladkrabang, Computer Engineering, Bangkok, Thailand

Abstract

Multi-wavelength generation system using an optical spin within the modified add-drop optical filter known as a PANDA ring resonator for molecular transport network security is proposed. By using the dark-bright soliton pair control, the optical capsules can be constructed and applied to securely transport the trapped molecules within the network. The advantage is that the dark and bright soliton pair (components) can securely propagate for long distance without electromagnetic interference. In operation, the optical intensity from PANDA ring resonator is fed into gold nano-antenna, where the surface plasmon oscillation between soliton pair and metallic waveguide is established.

Keywords: molecular network, magnetic networks, spin networks, spin transport network

Introduction

Optical spin has been recognized as the promising key for future digital and computing technologies, which can be used for many applications such as semiconductors (Myers et al. 2008), magnetic tunnel junctions (Gordon et al. 2009), nano-antenna (Thammawongsa et al. 2012), thin-film nano-magnets (Ozatay et al. 2008), and cell communications (Meyl 2012). Till date, the optical excitation of nanoparticle with circularly light is an interesting idea, in which light pulse is used for spin generation and detection (Lampel 1986). By using the optical orientation (Galvez et al. 2007), the angular momentum of light is converted to be electronic spin and vice versa, which is very efficient in semiconductors. The consequence of this effect assists as an important aspect of spintronics, where it is used to spin-polarize electrons. These techniques were used to explain the behavior of paramagnetic ion resonance in quantum geometric confinement, where the optical spin resonance and transverse spin relaxation in magnetic semiconductor quantum wells are generated and achieved (Crooker et al. 1997). Moreover, the optical spin manipulation in electrically pumped vertical-cavity surface-emitting lasers is analyzed (Hövel et al. 2008), where the output polarization for mixed electrical and optical excitations is demonstrated. After that, the spin magnetic state and the static magnetic field were used to build the AND, OR, XOR (CNOT), and NAND gates by optical spin manipulation (Hübner et al. 2009). Optical spin generation using dark-bright soliton pair by PANDA ring resonator was proposed by Yupapin and his colleagues (Muhammad et al. 2012, Glomglome et al. 2012) that generate soliton pair called "soliton spin" (photonic spin) for optical communication system.

Recently, molecular communication has become a new communication pattern based on biological mechanism, which is used to encode molecules as information carrier. The most promising technique is one that converts molecular signal into optical information and transports the molecular information into a nano networking channel (Parcerisa et al. 2009). The important aim to develop molecular communication is to design and control the nano network devices that can transport the biological information, for instance, a number of techniques were shown such as molecular array and network (Atakan et al. 2012, Nakano et al. 2012) and multi-wavelength transportation by dark-bright soliton (Sarapat et al. 2009) and other applications (Amiri and Ali 2013, Amiri et al. 2013a, 2013b, 2013c, 2013d, Amiri and Ali 2014).

In this paper, Multi-wavelength molecular capsules for molecular transport network security are generated, which can be formed by optical spins, in which a dark-bright soliton pair is used to generate the high magnetic field using the gold nano-antenna coating, which is applied on device surface. The obtained results have shown that the soliton spin rotation and the spin sets can be obtained. In application, the molecular transport network security with soliton spin may be useful for molecular communication network, where the use of such a system for molecular nanosensor, molecular transportation, and optical spin cryptography can be realized.

Background

In this study, a modified add-drop filter called "PANDA" ring resonator which consists of add-drop filter (Rad)

Correspondence: Preecha P. Yupapin, King Mongkut's Institute of Technology Ladkrabang, Computer Engineering, Bangkok, 10520 Thailand. E-mail: kypreech@kmitl.ac.th

(Received 11 May 2014; revised 18 June 2014; accepted 26 June 2014)

coupled by two side microring (R1 and R2) being integrated together is proposed as shown in Figure 1. The orthogonal set of dark and bright soliton pair was generated by conversion process in the system which can be decomposed into left and right circularly polarized waves. Then, the add-drop optical filter device (Rth) with gold coating is connected that used to generate transverse magnetic field by spin polarization. Dark and bright optical solitons are provided, which are input into the Input and Add ports as shown in Eqs. (1) and (2), respectively (Sarapat et al. 2009, Agrawal 2007).

$$E_{\text{in1}}(t) = A\tanh\left[\frac{T}{T_0}\right]\exp(\text{M}), \tag{1}$$

$$E_{\text{add}}(t) = A\,\text{sech}\left[\frac{T}{T_0}\right]\exp(\text{M}), \tag{2}$$

Where $\text{M} = \left[\left(\frac{x}{2L_{\text{D}}}\right) - i\phi\omega_0(t)\right]$,

A is the amplitude of optical field and x is a distance propagation, T is a soliton pulse propagation time in a moving frame at group velocity, $T = t - \beta_1 x$, t is the soliton phase shift time, T_0 is soliton pulse propagation time at initial input, $LD = T_0^2/|\beta_2|$ is the dispersion length of the soliton pulse, where β_1 and β_2 are the linear and second-order terms of Taylor expansion coefficients of the propagation constant, and ω_0 is the soliton frequency shift.

The input light temporal coherence function in terms of random phase is given by

$$\phi(t) = \phi_0 + \phi_{\text{NL}} = \frac{2\pi n_2 L}{A_{\text{eff}}}|E_0(t)|^2, \tag{3}$$

Where ϕ_0 and ϕ_{NL} are linear and nonlinear phase shifts respectively, n_2 is the waveguide nonlinear refractive index, A_{eff} is the effective mode core area of the device, $L = 2\pi R_{\text{ad}}$, R_{ad} is the ring radius, $E_0(t)$ is the circulated field within the coupled ring resonator. In terms of the dark-bright soliton pulse, it is described as a solution which retains its temporal width invariance when it propagates. The nonlinear refractive index (n) of light propagates within the waveguide is given by

$$n = n_0 + n_2 I = n_0 + \frac{n_2}{A_{\text{eff}}}P, \tag{4}$$

Where n_0 and n_2 are the linear and nonlinear refractive indices, respectively, I is the optical intensity, P is the optical power (Kokubun et al. 2005, Fietz et al. 2007). Methodically, the soliton light pulse passes through the waveguide of the PANDA ring resonator system (Phatharaworamet et al. 2010), in which the input port provides the first coupled energy into the PANDA ring multiplexing system.

Therefore, the transmitted and circulated optical field components can be described by

$$E_{\text{T}} = Y_1\left[X_1 E_{\text{in1}} + \sqrt{k_1}E_4\right], \tag{5}$$

$$E_1 = Y_1\left[X_1 E_4 + \sqrt{k_1}E_{\text{in1}}\right], \tag{6}$$

$$E_2 = E_{R2}E_1\exp\left[-\frac{a}{2}\frac{L}{2} - jk_{\text{n}}\frac{\text{L}}{2}\right], \tag{7}$$

Where $Y_1 = \sqrt{1-\gamma_1}$, $X_1 = \sqrt{1-k_1}$.

The Add port pulse supply for a second coupler is given by

$$E_{\text{D}} = Y_2\left[X_2 E_{\text{add}} + \sqrt{\kappa_2}E_2\right], \tag{8}$$

$$E_3 = Y_2\left[X_2 E_2 + \sqrt{\kappa_2}E_{\text{add}}\right], \tag{9}$$

$$E_4 = E_{R1}E_3\exp\left[-\frac{a}{2}\frac{L}{2} - jk_n\frac{L}{2}\right], \tag{10}$$

Where $Y_2 = \sqrt{1-\gamma_2}$, $X_2 = \sqrt{1-k_2}$, k_1 and k_2 are the intensity coupling coefficients, γ_1 and γ_2 are the fractional coupling intensity losses, α is the waveguide attenuation coefficient, $k_{\text{n}} = 2\pi/\lambda$ is the wave propagation number, E_{R1} and E_{R2} are the optical field circulated components of the left and right microring, R_1 and R_2 are the ring radii of the left and right sides of the PANDA ring multiplexing system, respectively. The circulated optical field components E_{R1} and E_{R2} in the microring are given by

$$E_{R1} = E_3\left\{\frac{\left[\sqrt{Y_4X_4} - Y_4\right]\exp-\left(\frac{a}{2}L_1 - jk_nL_1\right)}{\left[1-\sqrt{Y_4X_4}\right]\exp-\left(\frac{a}{2}L_1 - jk_nL_1\right)}\right\}, \tag{11}$$

$$E_{R2} = E_1\left\{\frac{\left[\sqrt{Y_3X_3} - Y_3\right]\exp-\left(\frac{a}{2}L_2 - jk_nL_2\right)}{\left[1-\sqrt{Y_3X_3}\right]\exp-\left(\frac{a}{2}L_2 - jk_nL_2\right)}\right\}, \tag{12}$$

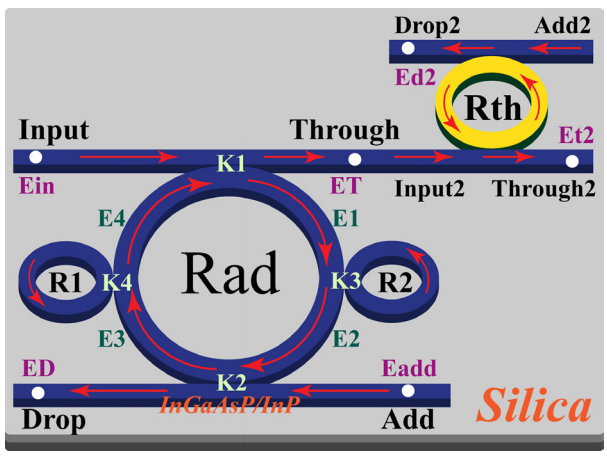

Figure 1. Schematic of multi-wavelength optical spins generated by soliton pulse in a PANDA ring resonator.

Where $Y_3 = (1-\gamma_3)$, $Y_4 = (1-\gamma_4)$, $X_3 = (1-k_3)$, $X_4 = (1-k_4)$, k_3 and k_4 are the intensity coupling coefficients, γ_3 and γ_4 are the fractional coupling intensity losses, $L_1 = 2\pi R_1$, R_1 is the left microring radius and $L_2 = 2\pi R_2$, R_2 is the right microring radius.

The output optical field (E_T) and the output power (P_T) of the through port are given by

$$E_T = x_1 y_1 E_{\text{in1}} + \left(j x_1 x_2 y_2 \sqrt{k_1} E_{R2} E_{R1} E_1 - x_1 x_2 \sqrt{k_1 k_2} E_{R1} E_{\text{add}} \right) \exp(TP) \quad (13)$$

$$P_T = (E_T)\cdot(E_T)^* = \left| x_1 y_1 E_{\text{in1}} + \left(j x_1 x_2 y_2 \sqrt{k_1} E_{R2} E_{R1} E_1 - x_1 x_2 \sqrt{k_1 k_2} E_{R1} E_{\text{add}} \right) \exp(\text{TP}) \right|^2 \quad (14)$$

The output optical field (E_D) and the output power of the drop port (P_D) are expressed by

$$E_D = x_2 y_2 E_{\text{add}} + j x_2 \sqrt{k_2} E_{R2} E_1 \exp(\text{TP}), \quad (15)$$

$$P_D = (E_D)\cdot(E_D)^* = \left| x_2 y_2 E_{\text{add}} + j x_2 \sqrt{k_2} E_{R2} E_1 \exp(\text{TP}) \right|^2, \quad (16)$$

Where $TP = -\frac{a}{4}\frac{L}{4} - jk_n \frac{L}{4}$

In order to retrieve the required signals, the proposed system is employed by the add-drop optical multiplexing device, where the electric field (E_{t2}) and light pulse output power (P_{t2}) are given by

$$E_{t2} = E_{t1} \frac{-X_5 \exp\left[-\frac{a}{2} L_b - jk_n L_b\right] + X_5}{1 - X_5 X_6 \exp\left[-\frac{a}{2} L_b - jk_n L_b\right]}, \quad (17)$$

$$P_{t2} = \left| \frac{E_{t2}}{E_{t1}} \right|^2 = \frac{(1 - k_5 - 2X_5 X_6 \exp P\, X \cos(k_n L_b) + (1-k_5)\exp P)}{(1 + (1-k_5)(1-k_6)\exp P - 2X_5 X_6 \exp P \cos(k_n L_b))} \quad (18)$$

The electric field, E_{d2} and the light pulse output power, P_{d2} are expressed by

$$E_{d2} = E_{t1} \frac{-\sqrt{k_5 k_6} \exp\left[-\frac{a}{2}\frac{L_b}{2} - jk_n \frac{L_b}{2}\right]}{1 - X_5 X_6 \exp\left[-\frac{a}{2} L_b - jk_n L_b\right]}, \quad (19)$$

$$\left(P_{d2} = \left| \frac{E_{d2}}{E_{t1}} \right|^2 = \frac{k_5 k_6 \exp P}{(1 + (1-k_5)(1-k_6)\exp P - 2X_5 X_6 \exp P \cos(k_n L_b))} \right), \quad (20)$$

Given $X_5 = \sqrt{1-k_5}$, $X_6 = \sqrt{1-k_6}$, and $P = \left[-\frac{\alpha}{2} L_b\right]$

Where k_5 and k_6 are the intensity coupling coefficients, $L_b = 2\pi R_b$, R_b is radius of add-drop optical multiplexing device as shown in Figure 1.

Multi-wavelength optical spins

In simulation, the parameters of add-drop optical multiplexer and both microrings on the left and right hand sides of the PANDA ring for MATLAB simulation are listed in Table I. The waveguide is made of ***InGaAsP/InP***, in which the refractive index value is 3.14 (Zhu et al. 2010, Mikroulis et al. 2008), where the wavelength is defined to be at $\lambda_0 = 1400$, 1425, 1450, 1475, 1500, 1525, 1550, 1575, 1600 nm. In the PANDA ring section, a dark soliton light pulse with 10 mW peak power is input into the input port, while a bright soliton with 1 mW peak power is fed into the Add port to control the device function. Afterward, the dark and bright soliton pulses are fed into Through port and circulated within the system; a flow diagram is shown in Figure 1, where finally the optical field is obtained at E_1, E_2, E_3, and E_4 positions as illustrated in Figure 2. The Through port (spin up) and Drop port (spin down) soliton spins are obtained in Figure 3. As a result, it is shown that many soliton spins can be produced from PANDA ring resonator. Therefore, the soliton spin array can be generated and controlled by the proposed system, which offers the required multi-wavelength optical spin generation.

Table I. List of waveguide and system parameters.

	R_{ad}	R_1	R_2	R_{th}	k_1	k_2	k_3	k_4	k_5	k_6	A_{eff} (μm^2)	n_0	α (dBmm^{-1})	γ
Waveguide parameters	30 µm	2.5 µm	2.5 µm	15 µm	0.5	0.5	0.3	0.3	0.5	0.5	0.25	3.34	0.1	0.01

Variable parameters	E_1 - E_4	E_{R1}	E_{R2}	E_T	E_D	E_{t1}
	Center ring electric fields	Left ring electric fields	Right ring electric fields	Through port electric fields	Drop port electric fields	Through add-drop electric fields
	E_{d1}	P_T	P_D	P_{t1}	P_{d1}	I
	Drop port add-drop electric fields	Through port optical power	Drop port optical power	Through add-drop optical power	Drop port add-drop optical power	Optical intensity
	L_D	L_{NL}	ϕ_{NL}	x	A	T
	Dispersion length	Nonlinear Dispersion length	Nonlinear Phase shift	Propagation distance	Optical amplitude	Propagation time

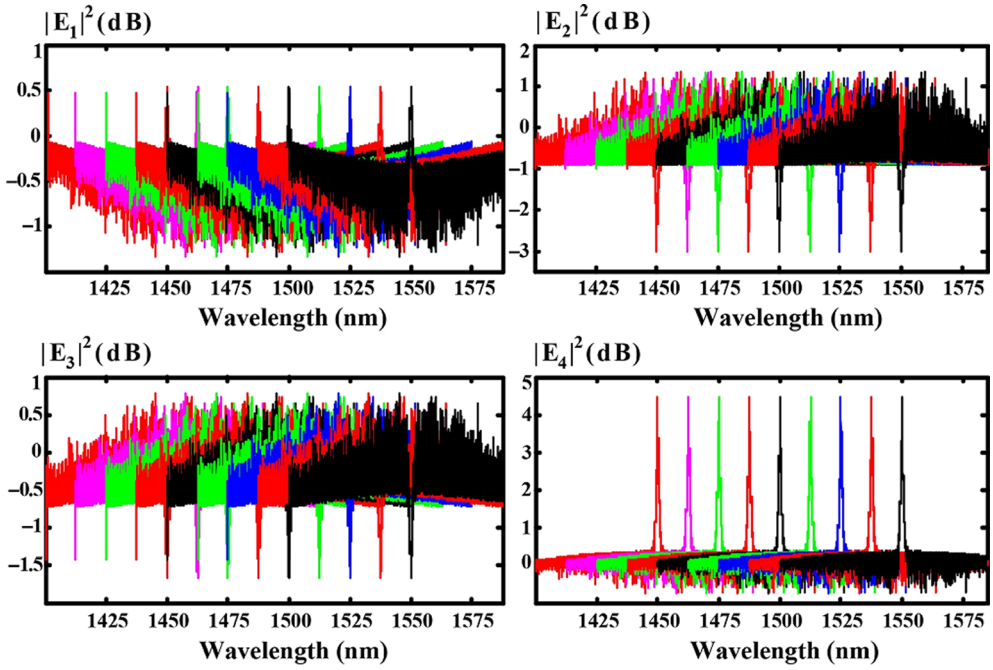

Figure 2. Many soliton spins within a PANDA ring are generated using a dark-soliton pump input at center wavelength 1400, 1425, 1450, 1475, 1500, 1525, 1550, 1575, and 1600 nm.

Figure 4 shows the 3D drawing of ring laterally gold coupled to the straight waveguides in Figure 4a and the cross section of add-drop in Figure 4b. The ring was coated by gold on the top as a nano-antenna, where the surface plasmonic resonance is produced, in which the output spin states can be confirmed by using the output polarizing beamsplitter arrangement. The dark-bright soliton conversion pulses within a PANDA ring resonator is generated and transmitted to gold coupled add-drop multiplexer, in which the multiplexed optical spins can be obtained and propagated into the provided network. Figure 5 shows the results of many spins by the proposed add-drop optical filter device which is coated by gold nano-antenna. A nano-antenna's current density is established by using the Pocklington's integral equation (Pocklington 1897). The complex one dimensional current density is calculated using MATLAB program (Biagioni et al. 2012), where the antenna input impedance is expressed by the simplify impedance, which is transmitted at different lengths (Balanis 1992). Generally, the gold (Au) material is the most popular material used for nano-antenna, which can provide a good effective resonance and dielectric constant values. The surface plasmon resonance of the interface between add-drop optical device and nano-antenna in terms of dispersion relation is described by using the Drude model (Rakic et al. 1998) as in following details.

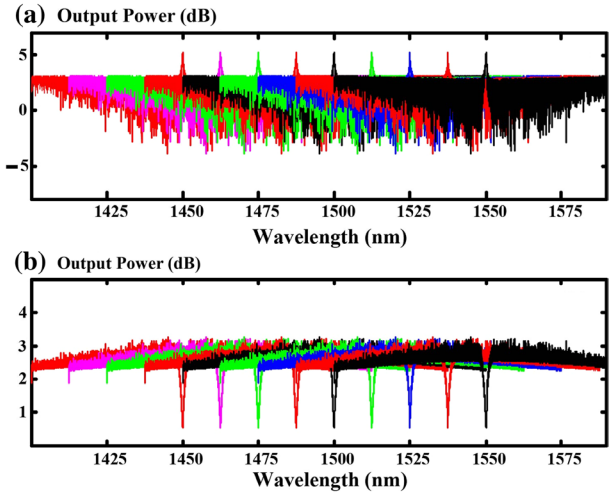

Figure 3. A set of spins obtained at (a) Through port (spin up) and (b) Drop ports (spin down).

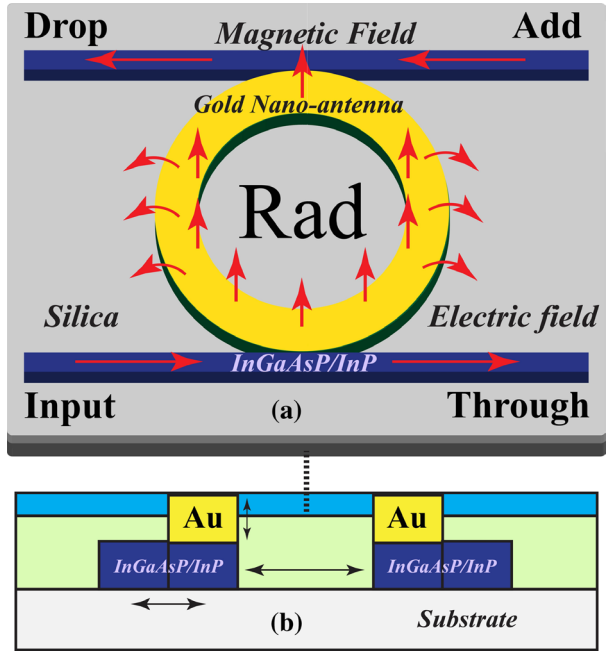

Figure 4. (a) 3D drawing of ring laterally gold coupled to the straight waveguides (b) and cross section of add-drop.

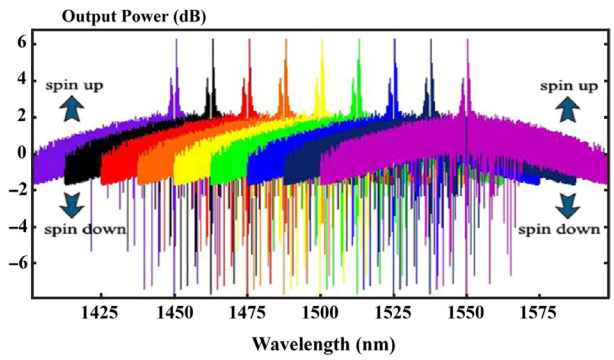

Figure 5. A set of spins obtained at Through and Drop ports of the Rth Add-Drop (Yupapin et al. 2013).

$$\varepsilon_m(\omega) = \varepsilon_1 + i\varepsilon_2, \tag{21}$$

$$\varepsilon_1(\omega) = 1 - \frac{\omega_p^2}{\omega^2 + \Gamma^2}, \tag{22}$$

$$\varepsilon_2(\omega) = \frac{\Gamma\omega_p^2}{\omega(\omega^2 + \Gamma^2)}, \tag{23}$$

Where $\omega_p = 2\pi f = 1.36 \times 10^{16}$rad s^{-1} and $\Gamma = 1.05 \times 10^{14}$rad s^{-1} are the size and temperature dependent plasma and collision frequency (f) of the nanoparticles, respectively. The intensity of surface plasmon resonance is improved when there is increase in the photothermal conversion process efficiency. Therefore, the extinction metal nanoparticle cross section given in Mie theory is derived by

$$E(\omega) = \frac{24\pi R \varepsilon_m^{3/2}}{\lambda} \frac{\varepsilon_2(\omega)}{(\varepsilon_1(\omega) + 2\varepsilon_m)^2 + \varepsilon_2^2(\omega)} \tag{24}$$

Where R is the radius of the ring and λ is the wavelength of the light in media, ω is the angular frequency of the exciting light, c is the velocity of light in vacuum, $\varepsilon_m(\omega)$ is the dispersive relative permittivity of the metal and math type is the dielectric functions of material. The surface plasmons oscillation is obtained by using a longitudinal electric field w, where TM-polarization and exponential decay of electric field are calculated by the Maxwell equations. The surface plasmon propagation constant (K_p) of the wave propagating along the metal-dielectric interface is given by

$$k_p = k_0 \sqrt{\left(\frac{\varepsilon_d \, \varepsilon_m(\omega)}{\varepsilon_d + \varepsilon_m}\right)}. \tag{25}$$

Where κ_0 is the wave vector in air, ε_d is the relative permittivity of the dielectric constant. This wave can be optically excited using a coupling coated by a thin gold film (Kretschmann configuration), whereas a TM-polarized light beam is imposed on the gold face under total internal reflection conditions. The user add-drop filters are employed to retrieve the required signals, where the different wavelength signals (spins) can be obtained using the wavelength selectors (add-drop filters) at the end of the drop port. On the other hand, the modified data can be input into the network via the add port of each user in the transmission networks, which is shown in Figure 6. The received signals of each user (1–4) from add-drop filters at the through and drop ports are shown Figures 7 and 8, in which the spin wavelength selectors are employed as the key instrumental components. The certain or a narrow band wavelength can be obtained before the required spin signals are being detected via the end users. In terms of signal quality, the simulated free spectral range (FSR) transmission = 25 nm and full width half maximum (FWHM) = 4 nm are achieved as shown in Figure 9, where the output optical spins with different wavelengths can be obtained.

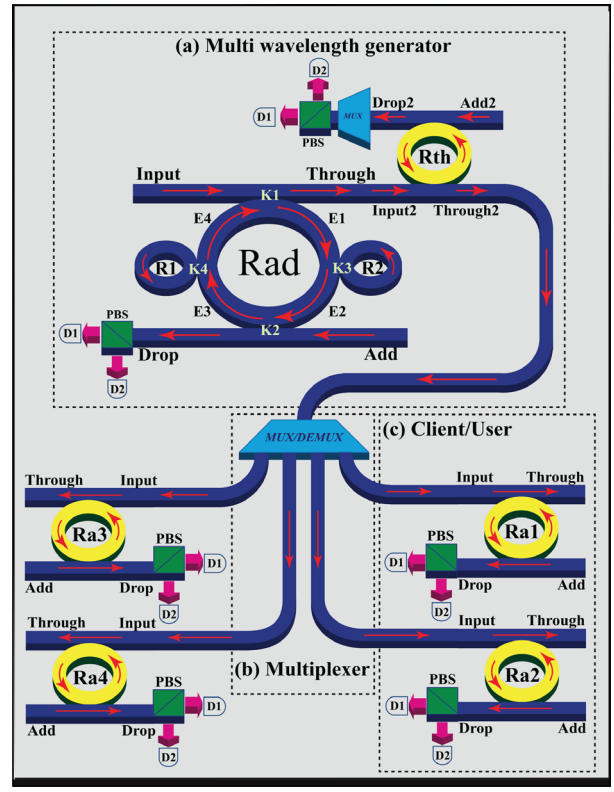

Figure 6. A schematic diagram of spin distributed networks using the multi-wavelength optical spins, where D1: detectors, PBS: polarizing beamsplitter, Rgs: output ring radii (users).

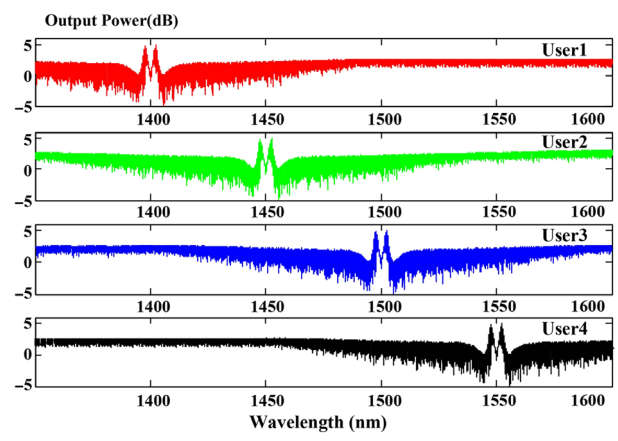

Figure 7. Results received by each user (1–4) from add-drop filter at Through port.

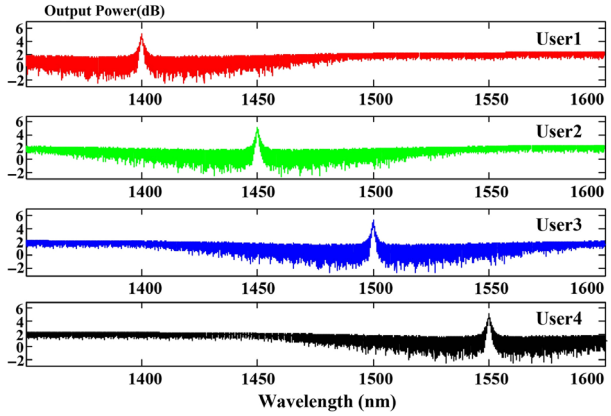

Figure 8. Results received by each user (1–4) from add-drop filter at Drop port.

In simulation, the optical spins and the magnetic fields can be generated by applying gold film coating, in which the magnetic induction on the device surface can be induced, as shown in Figure 4. Hence, the proposed system in Figure 8, a polarizing beam splitter (PBS) is used to distinguish the data and reference signals at the required destination in part (a). After that, data from the device enters into the multiplexing device (multiplexer, MUX) to encrypt data and transmit into the optical network. The generated multi-spins (many optical spins) can be used to form the wavelength division multiplexing data transmission, which offers the advantage of a long journey without interference and safely arrives at the destinations. Finally, the required signals can be retrieved (decoded by the demultiplexing, DEMUX) in part (b). After travelling through the DEMUX, the information will also be sent to the end users using the add-drop filters, in which the magnetic field is generated to identify the required data in part (c).

Generally, the long distance link means the soliton output power that can be useful for $>$1,000 km via an optical fiber link (Grigoryan et al. 2000), where the proposed system power of 10 dBm is obtained, which can be transmitted over 4,000 km for nine-channel transmission (Essiambre et al. 1997), while the time jitter in a soliton communication can be reduced by using the periodic optical phase conjugation (OPC) device (Parcerisa et al. 2009). By using the small waveguide effective area, the polarization-dependent loss of $<$0.1dB at 1550 nm can be achieved (Van Laere et al. 2009, Yang et al. 2009), where the spin detection can be realized in the form of polarization mode by using the polarizing beamsplitter and detected by the end users. The minimum detuning of the two signals (solitons) can be obtained, where in this case the detuning of 6.8 THz can be obtained between two signals (bands), where more detail can be found in reference (Yang et al. 2009). However, this is a simulation work in practice, if the propagation loss varies with wavelength, then the solitons away from the center (peak) wavelength (1500 nm) will not be valid for long distance propagation.

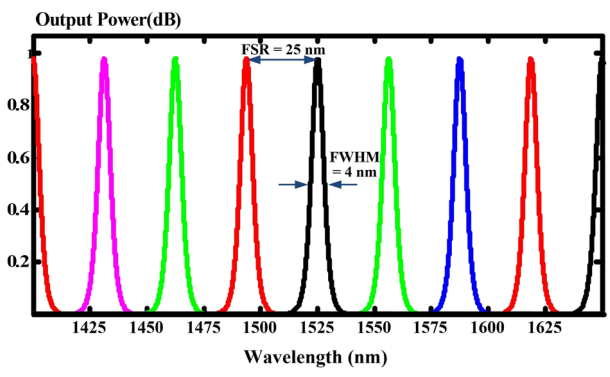

Figure 9. Simulated transmission FSR = 25 nm and FWHM = 4 nm.

Molecular network security

Molecular encapsulation network is the confinement of a molecule inside the cavity such as molecular capsule, molecular container or cage to transport along network. The essential suggestions are security and separation molecular capsules for specific destination.

In this model, we propose a network by using dark-bright soliton conversion control (Yupapin et al. 2013, Thammawongsa et al. 2013a) as shown in Figure 6, in which molecules (drug) can be trapped and moved securely along the network. The end users can perform the recovered molecules by using the molecular filter via the through port (Aziz et al. 2012), the transmission security can also be realized by using the soliton spin up-down coded and decoded (codec) technique via the drop port (Yupapin et al. 2014). Moreover, the optical spin states can be formed by polarization states via the polarizing beam splitter, while the state confirmation can be initialized by the transmitter (Alice) related to the receiver (Bob), where finally the security is confirmed by both parties. The optical capsules by soliton pair within the optical network for molecular delivery can securely trap the required molecules as shown in Figure 10, which is transmitted by the gradient force and scattering force as shown in Figure 10a. Finally, the specific codes between Alice and Bob can be recognized. The detached signals are shown in Figure 10b. In applications, the multi-wavelength optical spins network may be useful for network controls of molecular communication, switching, routing, and addressing at nano scale, coding in molecular networks, molecular networks security, nano computer networks, monitoring, and nano networks with larger-scale network integration.

Conclusion

In this work, multi-wavelength optical spin network system is proposed using the orthogonal dark-bright soliton conversion pulses within a PANDA ring resonator. The surface plasmonic resonance is induced by applying gold nano-antenna coating on the surface of the device. The coupling between the optical fields and the gold coating waveguide generates the transverse electric (TE) and magnetic field (TM) that can be separated using the add-drop filter and PBS for reference source and required signals at the destinations (end users). The results obtained have shown that multi-optical spins in the optical networks, i.e., spin networks (SpinNet) can be formed in which optical capsules by soliton pair within the optical network for molecular

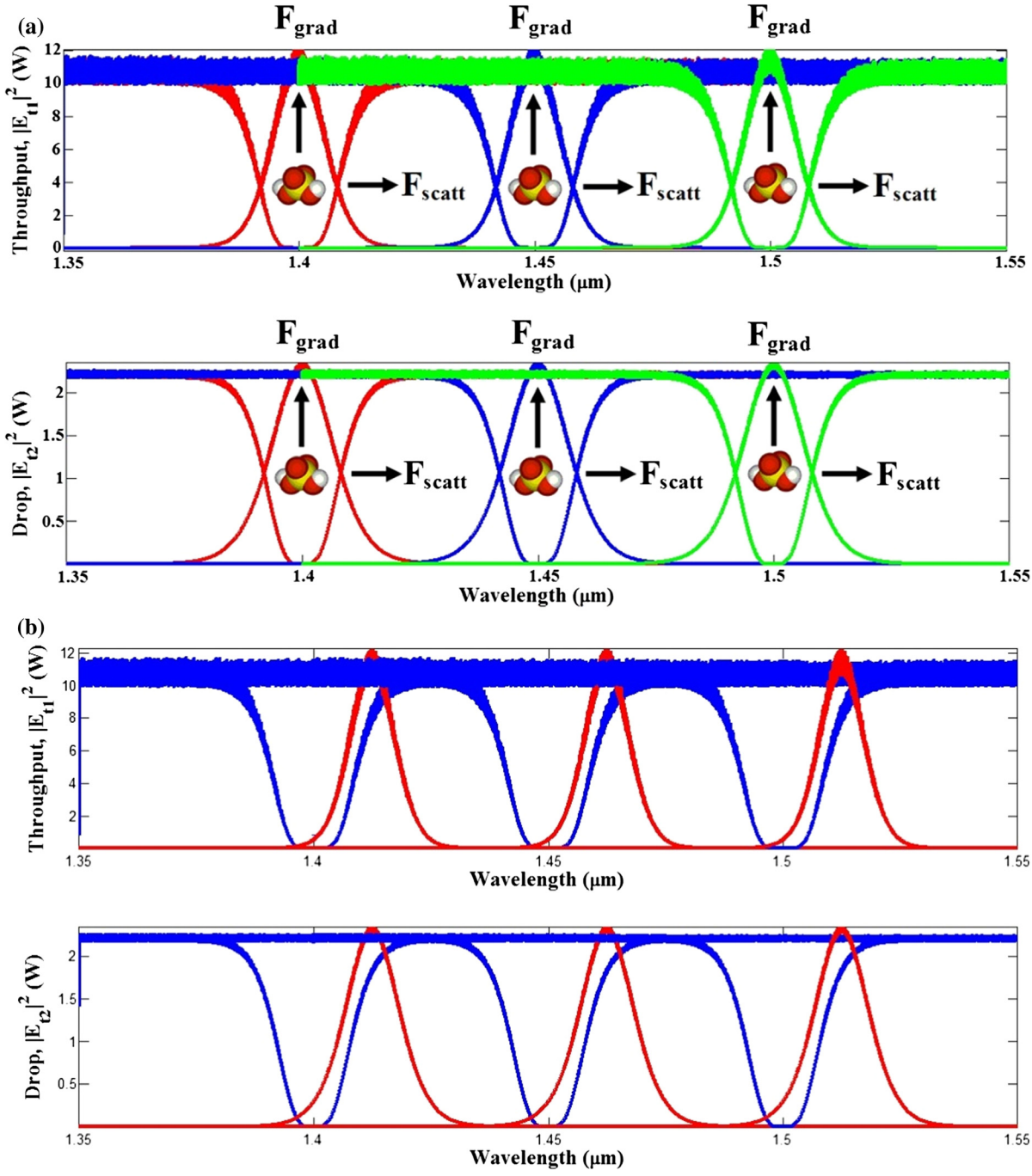

Figure 10. Schematic of trapped molecules within the optical capsules, (a) optical capsules, (b) open optical capsules; Fgrad: gradient force, Fscatt: scattering force.

delivery can securely trap the required molecules. The maximum force is given by Stokes' drag calibration that could be exerted on the particles, where the particle diameters ranging from 101 to 254 nm, the maximum force was found to be within the range of 0.56–2.2 pN, with a laser power of 135 mW. Therefore, the maximum force can be exerted into the proposed system by using the full laser power of 7 W, which will be around 20 pN, which can be found in ref (Thammawongsa et al. 2013b).

The advantage of the optical spin in network is absence of electromagnetic interference during propagation within the network. However, this is a small scale device and system, which gives the advantage for short range communication, where the multi-wavelength soliton spin may be of benefit for optical network communication and cryptography based spins, where the link loss can be assumed small. Moreover, the use of secure trapped molecules (drug) for long distance link can also be available by using the optical capsules, which can be useful for multi-access drug delivery with long distance link.

Acknowledgments

The author would like to acknowledge King Mongkut's Institute of Technology Ladkrabang (KMITL), Bangkok 10520, Thailand for the research laboratory facilities.

Declaration of interest

The authors report no declarations of interest. The authors alone are responsible for the content and writing of the paper.

References

Agrawal GP. 2007. Nonlinear Fiber Optics, 4th ed. San Diego, CA: Academic Press .

Amiri IS, Alavi SE, Ali J. 2013b. High-capacity soliton transmission for indoor and outdoor communications using integrated ring resonators. Int J Commun Syst.

Amiri IS, Alavi Sevia SE, Idrus M, Nikoukar A, Ali J. 2013a. IEEE 802.15.3c WPAN standard using millimeter optical soliton pulse generated by a Panda Ring Resonator. IEEE Photonics J. 5:7901912.

Amiri IS, Ali J. 2013. Data signal processing via Manchester coding-decoding method using chaotic signals generated by PANDA ring resonator. Chin Opt Lett. 11:041901.

Amiri IS, Ali J. 2014. Generating highly dark-bright solitons by Gaussian beam propagation in a panda ring resonator. J Comput Theor Nanosci. 11:1092–1099.

Amiri IS, Nikmaram M, Shahidinejad A, Ali J. 2013d. Generation of potential wells used for quantum codes transmission via a TDMA network communication system. Int J Commun Syst.

Amiri IS, Soltanmohammadi S, Shahidinejad A, Ali J. 2013c. Optical quantum transmitter with finesse of 30 at 800-nm central wavelength using microring resonators. Opt Quant Electron. 45:1095–1105.

Atakan B, Glames S, Akan OO. 2012. Nanoscale communication with molecular arrays in nanonetworks. IEEE Trans NanoBisci. 11:149–160.

Aziz MS, Daud S, Ali J, Yupapin PP. 2012. Molecular filter on-chip. J Biosens Bioelectron. 3:120–125.

Balanis CA. 1992. Antenna theory. Rev Process IEEE. 80:7–22.

Biagioni P, Huang JS, Hecht B. 2012. Nano antennas for visible and infrared radiation. Rep Prog Phys. 75:24402–24441.

Crooker SA, Awschalom DD. 1997. Optical spin resonance and transverse spin relaxation in magnetic semiconductor quantum wells. Phys Rev B Condens Matter. 56:7574–7587.

Essiambre RJ, Agrawal GP. 1997. Timing jitter of ultrashort solitons in high-speed communication systems. II. Control of jitter by periodic optical phase conjugation. J Opt Soc Am B. 14:323–330.

Fietz C, Shvets G. 2007. Nonlinear polarization conversion using microring resonators. Opt Lett. 32:1683–1685.

Galvez EJ, Zhelev N. 2007. Orbital angular momentum of light in optics instruction. J. Opt Soc Am B Opt Phys. 1:1–6.

Glomglome S, Srithanachai I, Teeka C, Mitatha S, Niemcharoen S, Yupapin PP. 2012. Optical spin generated by a soliton pulse in an add–drop filter for optoelectronic and spintronic, Opt Laser Technol. 44:1294–1297.

Gordon DF, Hafizi B, Ting A. 2009. Nonlinear conversion of photon spin to photon orbital angular momentum, Opt Lett. 34:3280–3282.

Grigoryan VS, Mu RM, Carter GM, Menyuk CR. 2000. Experimental demonstration of long-distance dispersion-managed soliton propagation at zero average dispersion. IEEE Photon Technol Lett. 12:45–46.

Hövel S, Bischoff A, Gerhardt NC, Hofmann MR, Ackemann T. 2008. Optical spin manipulation of electrically pumped vertical-cavity surface emitting Lasers, Appl. Phys Lett. 92:041118–3.

Hübner WH, Kersten S, Lefkidis G. 2009. Optical spin manipulation for minimal magnetic logic operations in metallic three-center magnetic clusters, Phys. Rev B: Condens Matter. 79:184431–184435.

Kokubun Y, Hatakeyama Y, Ogata M, Suzuki S, Zaizen N. 2005. Fabrication technologies for vertically coupled microring resonator with multilevel crossing busline and ultracompact ring radius. IEEE J Quantum Electron. 11:4–10.

Lampel G. 1986. Nuclear dynamic polarization by optical electronic saturation and optical pumping in semiconductors. Phys Rev Lett. 20:491–493.

Meyl K. 2012. Task of the introns, cell communication explained by field physics, J Cell Commun Signal. 6:53–58.

Mikroulis S, Roditi E, Syvridis D. 2008. Direct modulation properties of 1.55μm InGaAsP/InP microring lasers. J Lightwave Technol. 26:251–256.

Muhammad FD, Teeka C, Ali J, Yupapin PP. 2012. Optical spin manipulation using dark-bright soliton behaviors in a panda ring resonator. Microwave Opt Technol Lett. 54:987–990.

Myers RC, Mikkelsen MH, Tang JM, Gossard AC, Flatte ME, Awschalom DD. 2008. Zero-field optical manipulation of magnetic ions in semiconductors. Nat Mater. 7:203–208.

Nakano T, Moore MJ, Fang W, Vasilakos AV, Jianwei S. 2012. Molecular communication and networking: opportunities and challenges. IEEE NanoBiosci. 11:135–148.

Ozatay O, Gowtham PG, Tan KW, Read JC, Mkhoyan KA, Thomas MG, et al. 2008. Sidewall oxide effects on spin-torque and magnetic-field-induced reversal characteristics of thin-film nanomagnets. Nat Mater. 7:567–573.

Parcerisa L Akyildiz IF. 2009. Molecular communication options for long range nanonetworks. Comput Netw J. 53:2753–2766.

Phatharaworamet T, Teeka C, Jomtarak R, Mitatha S, Yupapin PP. 2010. Random binary code generation using dark-bright soliton conversion control within a PANDA ring resonator. J Lightwave Technol. 28:2804–2809.

Pocklington HC. 1897. Electrical oscillations in wires. Proc Cambridge Philos Soc. 9:324–332.

Rakic AD, Djuriic AB, Elazar JM. 1998. Optical properties of metallic films for vertical-cavity optoelectronic devices. Appl Opt. 37:5271–5283.

Sarapat K, Sangwara N, Srinuanjan K, Yupapin PP, Pornsuwancharoen N. 2009. Novel dark-bright optical solitons conversion system and power amplification. Opt Eng. 48:045004–7.

Thammawongsa N, Mitatha S, Yupapin PP. 2013a. Optical spins and nano-antenna array for magnetics therapy. IEEE Trans NanoBiosci. 13:228–232.

Thammawongsa N, Moongfangklang N, Mitatha S, Yupapin PP. 2012. Novel nano-antenna system design using photonic spin in a PANDA ring, PIER Lett. 31:75–87.

Thammawongsa N, Zainol FD, Mitatha S, Ali J, Yupapin PP. 2013b. Nanorobot controlled by optical tweezer spin for microsurgical use. IEEE Trans Nanotechnol. 12:29–34.

Van Laere F, Stomeo T, Cambournac C, Ayre M, Brenot R, Benisty H, et al. 2009. Nanophotonic polarization diversity demultiplexer chip. IEEE Photon Technol. 27:417–425.

Yang WX, Hou JM, Lin YY, Lee RK. 2009. Detuning management of optical solitons in coupled quantum wells. Phys Rev A. 79:033825.

Yupapin P, Ali J. 2014. Small Scale Optics. CRC Press: London.

Yupapin PP, Kulsirirat K, Techithdeera W. 2013. Optical capsule and tweezer for molecular motor use'. IEEE Trans NanoBiosci. 13:222–227.

Zhu J, Ozdemir SK, Xiao YF, Li L, He L, Chen DR, Yang L. 2010. On-chip single nanoparticle detection and sizing by mode splitting in an ultrahigh-Q microresonator. Nat Photonics. 32:1683–1685.